

Journal of Visualized Experiments

Biofunctionalization of Magnetic Nanomaterials

--Manuscript Draft--

Article Type:	Invited Methods Article - JoVE Produced Video
Manuscript Number:	JoVE61360R2
Full Title:	Biofunctionalization of Magnetic Nanomaterials
Section/Category:	JoVE Biochemistry
Keywords:	Nanomaterials, Magnetic, Nanomedicine, Antibody, APTES, Biocompatibility, Biofunctionalization, Nanotechnology, Iron Nanowires
Corresponding Author:	Nouf Alsharif King Abdullah University of Science and Technology thuwal, makkah SAUDI ARABIA
Corresponding Author's Institution:	King Abdullah University of Science and Technology
Corresponding Author E-Mail:	nouf.alsharif@kaust.edu.sa
Order of Authors:	Nouf Alsharif
	Jasmeen Merzaban
	Jürgen Kosel
Additional Information:	
Question	Response
Please indicate whether this article will be Standard Access or Open Access.	Open Access (US\$4,200)
Please indicate the city, state/province, and country where this article will be filmed . Please do not use abbreviations.	Thuwal, Saudi Arabia

TITLE:**Biofunctionalization of Magnetic Nanomaterials****AUTHORS & AFFILIATIONS:**

Nouf A. Alsharif¹, Jasmeen Merzaban², Jürgen Kosel^{1,2}

1. Division of Biological and Environmental Sciences and Engineering, King Abdullah University of Science and Technology, Thuwal Jeddah, Saudi Arabia

2. Division of Computer, Electrical and Mathematical Sciences and Engineering, King Abdullah University of Science and Technology, Thuwal Jeddah, Saudi Arabia

Email Addresses of Co-authors:

Jürgen Kosel: Jurgen.Kosel@kaust.edu.sa

Jasmeen Merzaban: jasmeen.merzaban@kaust.edu.sa

Corresponding Author:

Nouf Alsharif (Nouf.Alsharif@kaust.edu.sa)

KEYWORDS:

Nanomaterials, Magnetic, Nanomedicine, Antibody, APTES, Biocompatibility, Biofunctionalization, Nanotechnology, Iron Nanowires

SUMMARY:

In this work, we provide a protocol to biofunctionalize magnetic nanomaterials with antibodies for specific cell targeting. As examples, we utilize iron nanowires to target cancer cells.

ABSTRACT:

Magnetic nanomaterials have received great attention in different biomedical applications. Biofunctionalizing these nanomaterials with specific targeting agents is a crucial aspect to enhance their efficacy in diagnostics and treatments while minimizing the side effects. The benefit of magnetic nanomaterials compared to non-magnetic ones is their ability to respond to magnetic fields in a contact-free manner and over large distances. This allows to guide or accumulate them, while they can also be monitored. Recently, magnetic nanowires (NWs) with unique features were developed for biomedical applications. The large magnetic moment of these NWs enables a more efficient remote control of their movement by a magnetic field. This has been utilized with great success in cancer treatment, drug delivery, cell tracing, stem cell differentiation or magnetic resonance imaging. In addition, the NW fabrication by template-assisted electrochemical deposition provides a versatile method with tight control over the NW properties. Especially iron NWs and iron-iron oxide (core-shell) NWs are suitable for biomedical applications, due to their high magnetization and low toxicity.

In this work, we provide a method to biofunctionalize iron/iron oxide NWs with specific antibodies directed against a specific cell surface marker that is overexpressed in a large number of cancer cells. Since the method utilizes the properties of the iron oxide surface, it is also

applicable to superparamagnetic iron oxide nanoparticles. The NWs are first coated with 3-aminopropyl-tri-ethoxy-silane (APTES) acting as a linker, which the antibodies are covalently attached to. The APTES coating and the antibody biofunctionalization are proven by electron energy loss spectroscopy (EELS) and zeta potential measurements. In addition, the antigenicity of the antibodies on the NWs is tested by using immunoprecipitation and western blot. The specific targeting of the biofunctionalized NWs and their biocompatibility are studied by confocal microscopy and a cell viability assay.

INTRODUCTION:

A unique property of magnetic nanomaterials is their ability to respond to magnetic fields¹, which can be beneficially utilized to actuate them in many ways, while they can also be monitored, for instance, by magnetic resonance imaging (MRI). When applying an alternating magnetic field at high frequency, they can generate heat, which can induce hyperthermia, providing a therapeutic option¹. Another approach is photothermal treatment, which can be realized with a near infrared (NIR) laser^{2,3}.

Among the large number of magnetic nanomaterials, iron oxide has received the greatest attention in biological applications such as magnetic separation, hyperthermia^{2,4}, cell guidance⁵, drug delivery⁶⁻⁸, and as a contrast agent in MRI^{9,10}. This is due to their high biocompatibility^{11,12}, large magnetization^{11,12}, ability to be coated^{9,13-15}, ability to carry drugs^{2,16}, ability to be functionalized with drugs^{2,16} or/and targeting agents^{12,13,17,18}, and ability to convert optical energy to heat². Recently, MagForce started in clinical trials on cancer patients using iron oxide nanoparticles for hyperthermia treatment¹⁹.

Lately, magnetic nanowires (NWs) have been increasingly exploited for biomedical applications^{3,11,16,20-22}. They have similar properties as magnetic nanobeads, but offer an anisotropic shape and a very large magnetic moment, which enables a very efficient remote control by a magnetic field^{23,24}, including low-frequency actuation to induce magneto-mechanical effects²⁵⁻²⁹. As a consequence, the NWs have been implemented for different biological applications such as exosomes isolation³⁰, cell tracking²¹, cancer treatment^{3,11,16}, drug delivery^{16,31,32}, and as a MRI contrast agent³³.

Biofunctionalized magnetic nanomaterials with specific cell targeting ability have great potential for biomedical applications and in precision medicine^{34,35}. To attach these targeting agents, a surface modification is required on the nanomaterials. Typically, they need a coating that provides a functional group, which facilitates the attachment of the treating agents. In literature, there is a large number of organic and inorganic coatings for magnetic nanomaterials. Based on the functional group that can be immobilized to the nanomaterial, these coatings can be categorized in four main groups: molecules based on carboxylic acid groups, polymers, histidine, and molecules based on silane groups.

The molecules based on carboxylic acid groups are a surface modification method that utilizes the high affinity between the negative carboxylic acid group on the coating and the positive charge on the magnetic nanomaterials³⁶⁻³⁸. The binding process of a carboxylic acid to a metal

surface may involve the generation of metal-carboxylate salts or adhesion of the carboxyl group to the metal. However, for multi-segmented NWs, such as iron/gold or nickel/gold NWs, which have superb properties for bio-applications^{39,40}, this type of coating cannot be applied easily. It requires two different coatings at the same time: thiol groups for modifying the gold segments and carboxyl groups for magnetic segments (iron or nickel)³⁸. Some examples of molecules based on carboxyl groups are hematoporphyrin, pimelic acid, palmitic acid, and 3-[(2-aminoethyl) dithio] propionic acid (AEDP)³⁸. Surface modifications of magnetic nanomaterials using polymers offer some distinct advantages. Due to the large molecular weight of the polymers, it enhances the stability of the magnetic nanomaterial in a solution³⁸. However, it will significantly increase the size of the nanomaterial³⁸. Polyvinylpyrrolidone (PVP), polyethyleneimine (PEI), arginine-glycine-D aspartic acid (RGD), and polyethylene glycol (PEG) are some examples of the most commonly used polymers for surface modifications. Each one has its own features and uses³⁸. The third surface modification method is using a histidine coating. Histidine is a protein with a histidine amino acid side chain that has a high affinity to limited number of magnetic nanomaterials such as nickel³⁸. It can be employed for protein purification processes^{38,41,42}. A histidine coating can also be applied to multi-segmented NWs, such as nickel/gold NWs³⁸. The silanization of a nanomaterial surface is a well-established process^{38,43,44}. It is based on a silicon atom linked to any metal oxide surface through three single bonds, and at the same time this silicon atom is binding to the functional group at the end through an alkyl chain^{38,43,44}. The advantage of this coating is providing free amine groups, and it has the ability to coat both magnetic and non-magnetic materials^{38,45}, such as nickel and gold, respectively. Therefore, using molecules based on the silane group is a practical route for biofunctionalizing multi-segmented NWs. Some example of molecules based on silane groups are (3-aminopropyl) triethoxysilane (APTES) and (3-aminopropyl) trimethoxysilane (APTMS)^{38,45}.

The addition of a targeting agent to the coating can play a significant role in both diagnosis and treatment of diseased cells, and, at the same time, minimize the side effects on healthy tissues^{46,47}. The addition of a targeting agent on the surface of nanomaterials enhances both cellular selective binding and internalization through endocytosis receptors⁷. Without these targeting ligands, nanomaterials interact nonspecifically with cell membranes, which binds at a lower rate compared to the nanomaterials with the ligands⁴⁸. One of the challenges of targeting cancer tissues is their characteristic similarity to healthy tissues. Therefore, the success of targeting depends mainly on determining the appropriate ligand to use as a biological target^{49,50}. Various targeting agents have been employed to direct nanomaterials to cancer cells^{48,51} (e.g., CD44, due to its high expression in cancer cells compared to healthy cells⁵²⁻⁵⁵).

Targeting agents can be categorized into three main groups, based on the components they are made of and their complexity: aptamer-based targeting, ligand-based targeting, and antibody-based targeting. Aptamers are short chemically synthesized strands of DNA or RNA-oligonucleotides that are folded into two- and three-dimensional structures, making them capable of targeting a specific antigen, most often proteins⁵⁶. Ligand-based targeting includes peptides and short amino acid chains⁵⁷. Antibody-based targeting involves the use of a whole antibody, or antibody fragments, such as single-chain variable fragments or antigen-binding fragments⁵¹. Using this method has the advantage of possessing two binding sites with a high binding affinity to its specific target

antigen, which gives it an exceedingly high selectivity⁵⁸. The binding sites are analogous to a lock and the antigen to a key⁵⁸.

In this work, the NWs used were fabricated by electrodeposition onto aluminum oxide membranes, a method described in detail in a previous publication⁵⁹. The focus here, is on releasing these iron-iron oxide (core-shell) NWs from the membranes and biofunctionalizing them with specific antibodies to provide a targeting ability. The antibodies cannot bind directly to the iron-iron oxide NWs and require a linker. Coating the NWs with APTES provides free amine groups, enabling the covalent attachment via the carboxyl group on the antibodies (**Figure 1**). The advantage of the APTES coating is its ability to work for both magnetic²¹ and non-magnetic⁶⁰ materials, such as iron/gold or nickel/ gold NWs⁴⁵. All the coating and biofunctionalization steps explained in this protocol can be utilized with any iron/iron oxide nanomaterial, in general. Iron/iron oxide NWs were used here as an example. The results show that the antibody-functionalized NWs have a high antigenicity to specific cell surface receptors, which can be used for different applications. Examples include cell separation, drug delivery, specific cancer cell treatment using photothermal and/or magneto-mechanical treatments.

PROTOCOL:

CAUTION: Always consult all relevant material safety data sheets (MSDS) before use. Use all appropriate safety practices and personal protective equipment (safety glasses, gloves, lab coat, full length pants, closed-toe shoes). Perform all biological reactions in the biological fume hood.

NOTE: This protocol is intended to produce 2×10^{10} biofunctionalized NWs/mL equivalent to 0.36 mg of iron/mL coated with anti-CD44 antibodies with a density of 3×10^4 antibodies/NW. The iron-iron oxide (core-shell) NWs are 2.5 μm long and have a diameter of 41.5 nm.

1. Release of iron nanowires

NOTE: The fabrication process of the iron/iron oxide NWs was explained in detail in a previous publication⁵⁹.

1.1. On a cutting mat, cut the aluminum (Al) discs (**Figure 2A**) into small pieces (**Figure 2B**) using a single edge blade and a small hammer to fit into a 2 mL tube. Use tweezers to transfer the small Al pieces to the tube.

1.2. Fill the 2 mL tube, containing the small Al pieces, with 1 mL of 1 M sodium hydroxide (NaOH). Make sure all the Al pieces are covered with the NaOH.

1.3. Leave the solution working for 30 min at room temperature inside of a chemical fume hood.

1.4. Remove only the Al pieces using the tweezer and keep the released NWs (black clusters, **Figure 3A**) in the NaOH solution for an additional 30 min. Do not change the NaOH solution.

177
178 1.5. Collect the NWs by placing the 2 mL tube in a magnetic rack and wait for 2 min before
179 removing the old 1 M NaOH solution. Replace it with fresh NaOH solution.

180
181 1.6. Sonicate the 2 mL tube containing the NWs for 30 s and leave it for 1 h inside a chemical
182 fume hood.

183
184 1.7. Repeat steps 1.5-1.6 at least four times.

185
186 1.8. Wash the NWs by placing the 2 mL tube in the magnetic rack and wait for 2 min.

187
188 1.9. Discard the NaOH solution and replace it with 1 mL of absolute ethanol.

189
190 1.10. Sonicate the tube for 30 s.

191
192 1.11. Place the 2 mL tube in the magnetic rack and wait 2 min.

193
194 1.12. Discard the old absolute ethanol solution and replace it with 1 mL of fresh absolute
195 ethanol and sonicate for 30 s.

196
197 1.13. Repeat step 1.11 and 1.12 for at least four times.

198
199 1.14. Keep the NWs in 1 mL of absolute ethanol at room temperature until they are needed.

200
201 1.15. Measure the concentration of iron and hence the NWs by using inductively coupled
202 plasma mass spectrometry (ICP-MS).

203
204 NOTE: The protocol can be paused here. However, for long-time storage, do not release the NWs
205 from the Al template until needed. Keeping the released NWs precipitating in the ethanol for a
206 long time without frequent sonication will create aggregations that will need longer times of
207 sonication to be separated.

208 209 **2. Coating the nanowires with APTES**

210
211 NOTE: In this protocol, 100 μL of APTES solution (density of 0.946 g/mL^{61}) is enough to coat $1.6 \times$
212 $10^7 \text{ m}^2/\text{g}$ of NWs. If there is a change in the ratio or the mass of the nanomaterial, the APTES
213 volume should be adjusted accordingly.

214
215 2.1. Transfer the NWs from step 1.14 to a 5 mL glass tube using a 1 mL pipette.

216
217 2.2. To collect any NWs left in the 2 mL tube, wash the empty 2 mL tube twice by adding 1 mL
218 of absolute ethanol and transfer it to the 5 mL glass tube using a 1 mL pipette.

219
220 2.3. By using the pipette, take 100 μL of APTES and add it to the NW solution directly.

2.4. Vortex the 5 mL glass tube for 10 s.

2.5. Adjust the 5 mL glass tube on the clamp of a laboratory retort stand.

2.6. Place half of the 5 mL glass tube inside of the water of the ultrasonic bath and sonicate for 1 h.

2.7. Take out the 5 mL glass tube from the ultrasonic bath and add 400 μ L of deionized (DI) water followed by 20 μ L of 1 M NaOH (basic catalysis).

CAUTION: It is important to add the DI water first.

2.8. Adjust the 5 mL glass tube, as explained in steps 2.5-2.6, and sonicate for another 1 h.

2.9. Take out the 5 mL glass tube from the ultrasonic bath.

2.10. Place a magnet next to the glass tube for 5 min to collect the NWs.

2.11. Replace the supernatant with 1 mL of fresh absolute ethanol and sonicate for 10 s.

2.12. Repeat steps 2.10-2.11 four times.

2.13. Transfer all NWs suspended ethanol to a new 5 mL glass tube using a 1 mL pipette.

NOTE: The APTES coated NWs can be stored in a glass tube with ethanol until they are needed. The protocol can be paused here.

3. Biofunctionalization of the nanowires

3.1. Activating the antibodies

NOTE: To achieve approximately 3×10^4 parts of antibody/NW, use 30 μ L of antibody (1 mg/mL) per 0.1 mg of iron.

3.1.1. In a 2 mL tube, dissolve 0.4 mg of 3-3-dimethyl-aminopropyl carbodiimide (EDC) and 1.1 mg of sulfo-N-hydroxysulfosuccinimide (Sulfo-NHS) in 1 mL of 2-N-morpholino ethanesulfonic acid hydrate (MES) (pH 4.7).

NOTE: The EDC/sulfo-NHS mixture should be fresh and prepared before using.

3.1.2. In a new 2 mL tube, add 30 μ L of anti-CD44 antibody (1 mg/mL), 960 μ L of 0.1 M of phosphate buffered saline (PBS, pH 7), and 10 μ L of EDC/sulfo-NHS mixture (prepared in step 3.1.1), respectively.

3.1.3. Place the 2 mL tube in a tube shaker at 10 x *g* for 15 min at room temperature.

3.2. Preparation of the APTES coated nanowires

3.2.1. During the 15 min incubation in step 3.1.3, wash the NWs by placing a magnet next to the APTES coated NWs tube (from step 2.13) for 2 min to collect the NWs.

3.2.2. Discard the ethanol and replace it with 1 mL of 0.1 M PBS (pH 7), and then sonicate for 10 s.

3.2.3. Repeat step 3.2.1-3.2.2 four times.

3.2.4. Collect the NWs, as explained in step 3.2.1, and discard the 0.1 M PBS. Keep the NWs in the tube without any solution.

3.3. Attachment of the antibodies

3.3.1. Transfer all the activated antibody solution (prepared in step 3.1.3) to the NWs tube (prepared in 3.2.4) and sonicate for 10 s.

3.3.2. Place the glass tube in the rotator overnight at 4 °C.

3.3.3. Collect the NWs using a magnet as in step 3.2.1 and discard the supernatant.

3.3.4. Adding 1 mL of 2% bovine serum albumin (BSA) solution for 1 h at 4 °C to block the reaction.

3.3.5. Check the antigenicity of the antibody functionalized NWs, for example, using immunoprecipitation (IP) and western blot (WB) assays.

NOTE: For better results, use the biofunctionalized NWs in the IP, WB, or biocompatibility assay immediately after the blocking step.

4. Biocompatibility assay

NOTE: To study the biocompatibility of the NWs, various cell viability assays and different cell lines can be employed. The concentration of the NWs used here is based on a previous publication¹⁶. The cell seeding should be done one day before the NW biofunctionalization.

CAUTION: All the below steps should be done under the biosafety cabinet.

4.1. In a 96-well plate, seed nine wells with 4×10^4 of colon cancer cells (HCT116 cell line) suspended in McCoy's cell culture media (100 μ L/well) and place it inside the incubator overnight at 37 °C and 5% carbon dioxide (CO₂).

4.2. Wash the NWs (from step 3.3.4) with PBS by collecting them using a magnet as in step 3.2.1 and replace the old solution with 1 mL of 0.01 M PBS (pH 7). Repeat this step three times.

4.3. Wash the NWs (from step 4.2) with warmed McCoy's media by collecting them using a magnet as in step 3.2.1 and replace the old PBS with 1 mL of warmed McCoy's media. Repeat this step three times.

4.4. Collecting the NWs (from step 4.3) using a magnet as in step 3.2.1 and replace the 1 mL of warmed McCoy's media with 900 μ L of warmed McCoy's media. The NWs concentration should be 0.02 mg of NWs per mL.

4.5. Take the 96-well plate (from step 4.1) from the incubator to the biosafety cabinet.

4.6. Under the biosafety cabinet, discard the old media from the cells and replace it with 100 μ L of suspended NWs (prepared in step 4.4).

4.7. Shake the plate (prepared in step 4.6) by hand and then incubate it for 24 h inside the incubator at 37 °C and 5% CO₂.

4.8. The next day, take out the 96-well plate (prepared in step 4.7) from the incubator. Under the biosafety cabinet, add 11 μ L of the cell viability reagent (**Table of Materials**) to each well using the multiwall pipette.

4.9. Shake the plate with the plate shaker at a speed of 10 x *g* for 10 s.

4.10. Incubate the plate for 1 h in the incubator.

4.11. Take out the 96-well plate (prepared in step 4.10) from the incubator. Read the plate in the microplate reader (**Table of Materials**) by measuring the absorbance of the cell viability reagent (excitation 540 nm, emission 590 nm).

REPRESENTATIVE RESULTS:

It is important to cut the aluminum (Al) discs (**Figure 2A**) into small pieces (**Figure 2B**) to fit in the tube used. After adding 1 M NaOH to the Al pieces, a reaction should start immediately, which is observed by the creation of bubbles. If no reaction occurs in 1 min or if the reaction is very fast and the solution turns completely turbid with a white cloud, remove the old NaOH solution immediately and replace it with a fresh solution. Check the pH value of the NaOH solution. It should be pH>12. When the NWs are released from the Al pieces in the first 30 min with NaOH, the NWs (black clusters, **Figure 3A**) will be floating within the NaOH solution. In the last step of releasing the NWs, the solution should be homogeneous. No cluster of NWs should be there

(**Figure 3B**). If NWs were collected with a magnet for 3 min, the solution should be clear, and the NW pellet should be black (**Figure 3C**). If the pellet was gray, discard the tube and start again with a new Al sample.

During the releasing process, the NWs obtain a native iron oxide layer with around 5 nm thickness, which is similar to previous reports^{11,16,20}. This oxide layer has an important contribution to the biocompatibility¹⁶, functionalization^{16,18} and magnetic properties²⁰ of the NWs. However, keeping the NWs in their template (i.e., not releasing them) until needed will prevent them from any environmental effects on them. The average diameter and length of the NWs after the releasing process were 2.5 μm and 41.5 nm, respectively. The mass of a single NW can be calculated as explain in **Table 1** and it confirmed by inductively coupled plasma mass spectroscopy (ICP-MS). Here, each alumina disc contained around 0.3 mg of iron.

To reduce the aggregation of the NWs after releasing and enable further functionalization, the NWs were coated with APTES. This coating provides free amine groups and has the ability to coat both magnetic and non-magnetic materials^{39,45}, making it suitable for coating multi-segmented NWs such as iron/gold NWs. During the nanowires coating, it is important to focus on two things. First, calculate the needed volume from APTES molecules⁶² based on the surface area and the mass of the NWs. These calculations were presented in **Table 2**. Secondly, keep the nanowires in a continuous movement to prevent their agglomeration and the blocking of some parts of NW surfaces from APTES coating. For instance, in this protocol, the nanowires were incubated under the ultrasonic bath and rotator during the APTES coating and antibody functionalization, respectively. Each APTES molecule contains a silicon atom and a terminal functional amine group²¹. Therefore, electron energy-loss spectroscopy (EELS) maps can be used to confirm the presence of the APTES coating by showing silicon atoms (pink color) on the NW surface (**Figure 4A**). In contrast, the non-coated NWs show the iron atoms in bark blue (**Figure 4B**) and iron/oxygen mix atoms in light blue (**Figure 4B**). The corresponding EELS mapping of non-coated NWs (**Figure 4C,4D**) shows a higher intensity of iron vs. oxygen in the center (**Figure 4C**) than on the surface (**Figure 4D**), indicating an iron-iron oxide (core-shell) structure. The EELS mapping (**Figure 4C,4D**) was identified that the iron oxide layer on the NWs is Fe_3O_4 more than Fe_2O_3 , which is similar to a previous publication²⁰.

The antigenicity of the attached antibodies can be confirmed using the IP and WB assays, where a band can be observed on the positive sample but not on the negative controls (**Figure 5**). Note that to observe a clear band, do not use less than 0.1 mg of NWs/ 10×10^6 cells. BCA assay (**Table of Materials**) in combination with some calculations presented in **Table 3** was used to quantify the antibodies number on the NW.

Furthermore, the zeta-potential measurement was used to elucidate the surface functionalization. The terminal amine group on APTES reduced the negative charge of the non-coated NWs, as shown in **Figure 6**. The antibody-functionalized NWs also changed the charge compared to the APTES-coated NWs (**Figure 6**). All the zeta-potential measurements were done at pH 7.

The specific cell targeting of the antibody-functionalized NWs can be confirmed using confocal microscopy (**Figure 7**). The biocompatibility of any new nanomaterial should be tested before starting any application. Therefore, the cell viability assay was used, and it confirmed that the non-coated, APTES coated-, and antibody coated-NWs were biocompatible even with a high concentration (**Figure 8**).

FIGURE AND TABLE LEGENDS:

Figure 1: Schematic represents the coating and biofunctionalization method of the nanowires. (A) Coating iron NWs with APTES. (B) Activating the antibodies by using EDC + Sulfo-NHS, to have at the end (C) an antibody functionalized nanowire.

Figure 2: Iron deposited aluminum disc. (A) The aluminum disc before the cutting. (B) The red lines showed where to cut the disc.

Figure 3: Nanowire release steps. (A) Clusters of nanowires are floating in NaOH solution. The image was taken 10 min after adding the NaOH and after removing the Al membrane. (B) Nanowires suspended in ethanol. The photo was taken in the last releasing step, immediately after the sonication step. (C) Black nanowire pellet collected by a magnet.

Figure 4: Electron energy-loss spectroscopy (EELS) map. (A) APTES coated nanowire (APTES-NW). The blue and pink colors represent iron and silicon atoms, respectively. (B) Non-coated nanowire (NW). The dark blue and light blue colors represent the iron and iron/oxygen mix mapping, respectively. The corresponding EELS mapping of (C) the core and (D) the shell of the non-coated NWs.

Figure 5: Confirmation of functionalization and activity of antibody conjugated nanowires. The antigenicity of CD44-NWs was confirmed by using immunoprecipitation (IP) and western blot (WB). +Ve: represents the positive control (full cell lysate). -Ve: represents the negative control (only non-coated NW). – CD44 cells: represents cells that do not express CD44 antigen; + CD44 cells: represents colon cancer cells that express CD44 antigen. This is a representative blot of n = 3 independent experiments.

Figure 6: Zeta potential values for NWs, APTES-NWs, and antibody. The bars represent the mean \pm standard error.

Figure 7: Confocal microscopic images shows the specific targeting. CD44-NWs are shown attaching (A and C), while the Isotype-NWs (negative control) did not attach (B and D). The red, blue, and green colors represent the cell membrane, nucleus, and cluster of CD44-NWs, respectively. A and B are the bright field images of C and D, respectively.

Figure 8: Cell viability study of colon cancer cells (HCT116) incubated with different formulations of nanowires. The cells were treated with NWs after 24h of incubation and then incubated for 24h with the NWs. All the experiments were carried out inside an incubator at 37 °C. The bars represent the mean \pm standard error.

Table 1. Calculation of the iron NW mass.

Table 2. Calculation the number of APTES molecules required for NWs coating.

Table 3. Calculation of the number of antibodies on the nanowire.

DISCUSSION:

As with any nanomaterial fabrication and coating method, a high quality of the solutions used is required. The release (1 M NaOH) and functionalization (MES) solutions can be reused several times. However, checking their pH value before starting a new process is very important. In the release step, washing the NWs with NaOH should be carried out at least four times. The better the washing, the better the stability of the NWs and the less they are aggregate. The oxide layer enhances the stability of the NWs upon immersion in ethanol or water⁶³.

The diameter and the length of the NWs were affected after coating them with APTES and antibodies. Here, the diameter increased from 41.5 nm to 70 nm, and the length decreased from 2.5 μm to 1.6 μm , due to the sonication steps that break the NWs. Therefore, it is essential characterize the morphology of the NWs after the biofunctionalization step.

The attachment of the antibodies to the NWs relies on the covalent interaction between the amine group (on APTES) and the carboxyl group (on the antibody). Therefore, confirming the presence of the APTES coating is an important step, for which we used EELS mapping. The coating method is safe and straightforward. It does not need high temperatures or long incubation times. Also, APTES coating works as a linker to enable the covalent attachment of other antibodies or proteins that has a carboxyl group.

In the case of biofunctionalizing the NWs with an antibody, the antigenicity of the antibodies' binding sites after the biofunctionalization process can be affected. The IP and WB method can be used to investigate this issue. Using the biofunctionalization method mentioned in this protocol will allow the antibodies to bind to the NWs with high antigenicity to a specific cell receptor. Moreover, biofunctionalizing the NWs with antibodies added the ability to target the cells with the receptor of interest, CD44 here. This was confirmed by confocal microscopy. Although the biocompatibility of the uncoated NWs was high (>95%), adding APTES coating or antibodies to the NWs enhanced their biocompatibility 100%.

Further, the coating and biofunctionalization protocol is efficient, economical, and reproducible. It should be applicable to any other iron-iron oxide nanomaterial, whereby the concentration of both the coating and the attached antibodies should be optimized based on the surface area and the mass of the nanomaterial. This protocol can be done safely at ambient conditions in the general laboratory. The biofunctionalization has significantly enhanced the biocompatibility of the nanomaterial and their targeting ability. In general, the NWs are extremely promising materials for nanomedical applications (including multi-modal or combinatorial treatments, cell

detection or guidance, and biological sensing). Combined with biofunctionalization, as described here, specific cell targeting can be achieved for increased precision and efficacy.

ACKNOWLEDGMENTS:

Research reported in this publication was supported by the King Abdullah University of Science and Technology (KAUST).

DISCLOSURES:

The authors have nothing to disclose.

REFERENCES:

- 1 Dürr, S. et al. Magnetic nanoparticles for cancer therapy. *Nanotechnology Reviews*. **2** (4), 395-409 (2013).
- 2 Espinosa, A. et al. Duality of iron oxide nanoparticles in cancer therapy: amplification of heating efficiency by magnetic hyperthermia and photothermal bimodal treatment. *ACS Nano*. **10** (2), 2436-2446 (2016).
- 3 Martínez Banderas, A. I. et al. Iron-Based Core-Shell Nanowires for Combinatorial Drug Delivery, Photothermal and Magnetic Therapy. *ACS Applied Materials Interfaces*. (2019).
- 4 Das, R. et al. Tunable high aspect ratio iron oxide nanorods for enhanced hyperthermia. *The Journal of Physical Chemistry*. **120** (18), 10086-10093 (2016).
- 5 Chen, J. et al. Guidance of stem cells to a target destination in vivo by magnetic nanoparticles in a magnetic field. *ACS Applied Materials Interfaces*. **5** (13), 5976-5985 (2013).
- 6 Juneja, R., Roy, I. Iron oxide-doped niosomes as drug carriers for magnetically targeted drug delivery. *International Journal of Nanomedicine*. **13**, 7 (2018).
- 7 Aires, A. et al. Multifunctionalized iron oxide nanoparticles for selective drug delivery to CD44-positive cancer cells. *Nanotechnology*. **27** (6), 065103 (2016).
- 8 Trabulo, S., Aires, A., Aicher, A., Heeschen, C., Cortajarena, A. L. Multifunctionalized iron oxide nanoparticles for selective targeting of pancreatic cancer cells. *Biochimica et Biophysica Acta -General Subjects*. **1861** (6), 1597-1605 (2017).
- 9 Blanco-Andujar, C. et al. Design of iron oxide-based nanoparticles for MRI and magnetic hyperthermia. *Nanomedicine*. **11** (14), 1889-1910 (2016).
- 10 Hachani, R. et al. Polyol synthesis, functionalisation, and biocompatibility studies of superparamagnetic iron oxide nanoparticles as potential MRI contrast agents. *Nanoscale*. **8** (6), 3278-3287 (2016).
- 11 Contreras, M. F., Sougrat, R., Zaher, A., Ravasi, T., Kosel, J. Non-chemotoxic induction of cancer cell death using magnetic nanowires. *International Journal of Nanomedicine*. **10** 2141 (2015).
- 12 Perez, J. E. et al. in *Cytotoxicity* Ch. 12 (IntechOpen, 2018).
- 13 Kievit, F. M., Zhang, M. Surface engineering of iron oxide nanoparticles for targeted cancer therapy. *Accounts of Chemical Research*. **44** (10), 853-862 (2011).
- 14 Xu, H. et al. Antibody conjugated magnetic iron oxide nanoparticles for cancer cell separation in fresh whole blood. *Journal of Biomaterials*. **32** (36), 9758-9765 (2011).
- 15 Zhang, L., Dong, W.-F., Sun, H.-B. Multifunctional superparamagnetic iron oxide

nanoparticles: design, synthesis and biomedical photonic applications. *Nanoscale*. **5** (17), 7664-7684 (2013).

16 Martínez-Banderas, A. I. et al. Functionalized magnetic nanowires for chemical and magneto-mechanical induction of cancer cell death. *Scientific Reports*. **6** 35786 (2016).

17 Tian, Q. et al. Multifunctional Polypyrrole@ Fe₃O₄ Nanoparticles for Dual-Modal Imaging and In Vivo Photothermal Cancer Therapy. *Small*. **10** (6), 1063-1068 (2014).

18 Alsharif, N. A., Martínez-Banderas, A. I., Merzaban, J., Ravasi, T., Kosel, J. Biofunctionalizing Magnetic Nanowires Toward Targeting and Killing Leukemia Cancer Cells. *IEEE Transactions on Magnetics*. **2** (99), 1-5 (2018).

19 Ventola, C. L. Progress in nanomedicine: approved and investigational nanodrugs. *Journal of Pharmacy Therapeutics*. **42** (12), 742 (2017).

20 Ivanov, Y. P. et al. Tunable magnetic nanowires for biomedical and harsh environment applications. *Scientific Reports*. **6** 24189 (2016).

21 Margineanu, M. B. et al. Semi-automated quantification of living cells with internalized nanostructures. *Journal of Nanobiotechnology*. **14** (1), 4 (2016).

22 Jeon, Y. S. et al. Metallic Fe–Au Barcode Nanowires as a Simultaneous T Cell Capturing and Cytokine Sensing Platform for Immunoassay at the Single-Cell Level. *ACS Applied Materials Interfaces*. **11** (27), 23901-23908 (2019).

23 Lee, E. et al. Highly selective CD44-specific gold nanorods for photothermal ablation of tumorigenic subpopulations generated in MCF7 mammospheres. *Nanotechnology*. **23** (46), 465101 (2012).

24 Patel, N. S., Lago-Cachón, D., Mohammed, H., Moreno, J. A., Kosel, J. J. J. Iron Nanowire Fabrication by Nano-Porous Anodized Aluminum and its Characterization. *Journal of Visualized Experiments*. (152), e60111 (2019).

25 Rozhkova, E. A. et al. Ferromagnetic microdisks as carriers for biomedical applications. *Journal of Applied Physics*. **105** (7), 07B306 (2009).

26 Kim, D.-H. et al. Biofunctionalized magnetic-vortex microdisks for targeted cancer-cell destruction. *Nature Materials*. **9** (2), 165-171 (2010).

27 Kim, D.-H. et al. Mechanoresponsive system based on sub-micron chitosan-functionalized ferromagnetic disks. *Journal of Materials Chemistry*. **21** (23), 8422-8426 (2011).

28 Vitol, E. A., Novosad, V., Rozhkova, E. A. Multifunctional ferromagnetic disks for modulating cell function. *IEEE Transactions on Magnetics*. **48** (11), 3269-3274 (2012).

29 Vitol, E. A., Novosad, V., Rozhkova, E. A. Microfabricated magnetic structures for future medicine: from sensors to cell actuators. *Nanomedicine*. **7** (10), 1611-1624 (2012).

30 Lim, J. et al. Direct isolation and characterization of circulating exosomes from biological samples using magnetic nanowires. *Journal of Nanobiotechnology*. **17** (1), 1-12 (2019).

31 Shore, D. et al. Electrodeposited Fe and Fe–Au nanowires as MRI contrast agents. *Chemical Communications*. **52** (85), 12634-12637 (2016).

32 Martínez-Banderas, A. I. et al. Iron-Based Core–Shell Nanowires for Combinatorial Drug Delivery and Photothermal and Magnetic Therapy. *ACS Applied Materials Interfaces*. **11** (47), 43976-43988 (2019).

33 Martínez-Banderas, A. I. et al. Magnetic core–shell nanowires as MRI contrast agents for cell tracking. *Journal of Nanobiotechnology*. **18** (1), 1-12 (2020).

34 Zhu, L., Zhou, Z., Mao, H., Yang, L. Magnetic nanoparticles for precision oncology:

theranostic magnetic iron oxide nanoparticles for image-guided and targeted cancer therapy. *Nanomedicine*. **12** (1), 73-87 (2017).

35 Guleria, A., Priyatharchini, K., Kumar, D. in *Applications of Nanomaterials*. 345-389 (Elsevier, 2018).

36 Allara, D. L., Nuzzo, R. G. Spontaneously organized molecular assemblies. 2. Quantitative infrared spectroscopic determination of equilibrium structures of solution-adsorbed n-alkanoic acids on an oxidized aluminum surface. *Langmuir*. **1** (1), 52-66 (1985).

37 Allara, D. L., Nuzzo, R. G. Spontaneously organized molecular assemblies. 1. Formation, dynamics, and physical properties of n-alkanoic acids adsorbed from solution on an oxidized aluminum surface. *Langmuir*. **1** (1), 45-52 (1985).

38 Schrittwieser, S., Reichinger, D., Schotter, J. Applications, surface modification and functionalization of nickel nanorods. *Materials and Structures*. **11** (1), 45 (2018).

39 Lim, J., Choi, M., Lee, H., Kim, Y. H., Han, J. Y., Lee, E. S., Cho, Y. Direct isolation and characterization of circulating exosomes from biological samples using magnetic nanowires. *Journal of Nanobiotechnology*. **17** (1), 1 (2019).

40 Nemati, Z. et al. Magnetic Isolation of Cancer-derived Exosomes Using Fe/Au Magnetic Nanowires. *ACS Applied Nano Materials*. **3** (2), 2058-2069 (2020).

41 Hainfeld, J. F., Liu, W., Halsey, C. M., Freimuth, P., Powell, R. D. Ni-NTA-gold clusters target His-tagged proteins. *Journal of Structural Biology*. **127** (2), 185-198 (1999).

42 Agarwal, G., Naik, R. R., Stone, M. O. Immobilization of histidine-tagged proteins on nickel by electrochemical dip pen nanolithography. *Journal of the American Chemical Society*. **125** (24), 7408-7412 (2003).

43 Aswal, D., Lenfant, S., Guerin, D., Yakhmi, J., Vuillaume, D. Self assembled monolayers on silicon for molecular electronics. *Analytica Chimica Acta*. **568** (1-2), 84-108 (2006).

44 Haensch, C., Hoepfner, S., Schubert, U. S. Chemical modification of self-assembled silane based monolayers by surface reactions. *Chemical Society Reviews*. **39** (6), 2323-2334 (2010).

45 Wildt, B., Mali, P., Searson, P. C. Electrochemical template synthesis of multisegment nanowires: Fabrication and protein functionalization. *Langmuir*. **22** (25), 10528-10534 (2006).

46 Schladt, T. D., Schneider, K., Schild, H., Tremel, W. Synthesis and bio-functionalization of magnetic nanoparticles for medical diagnosis and treatment. *Dalton Transactions*. **40** (24), 6315-6343 (2011).

47 Kumar, C. S. *Magnetic nanomaterials*. (John Wiley & Sons, 2009).

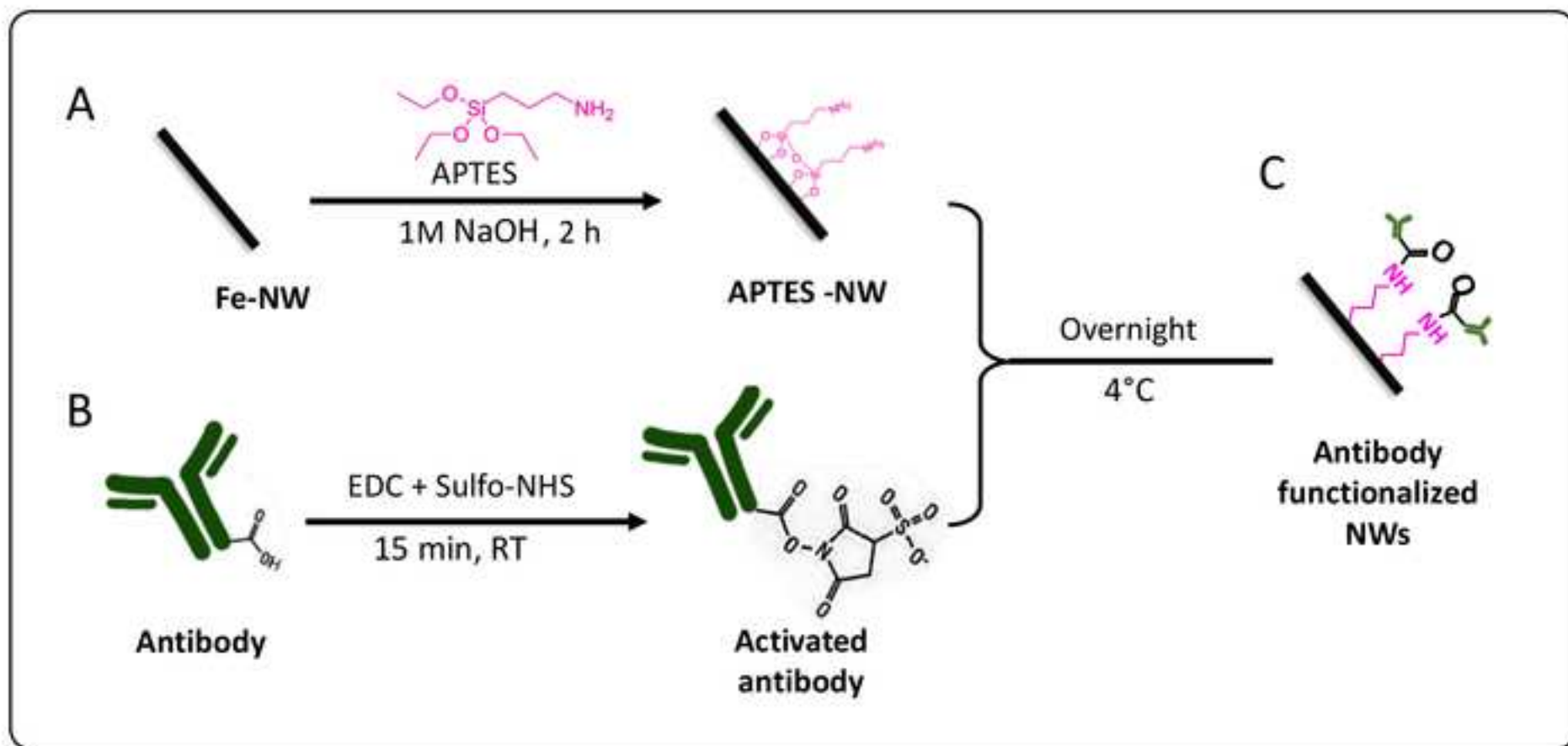
48 Peiris, P. et al. Precise targeting of cancer metastasis using multi-ligand nanoparticles incorporating four different ligands. *Nanoscale*. **10** (15), 6861-6871 (2018).

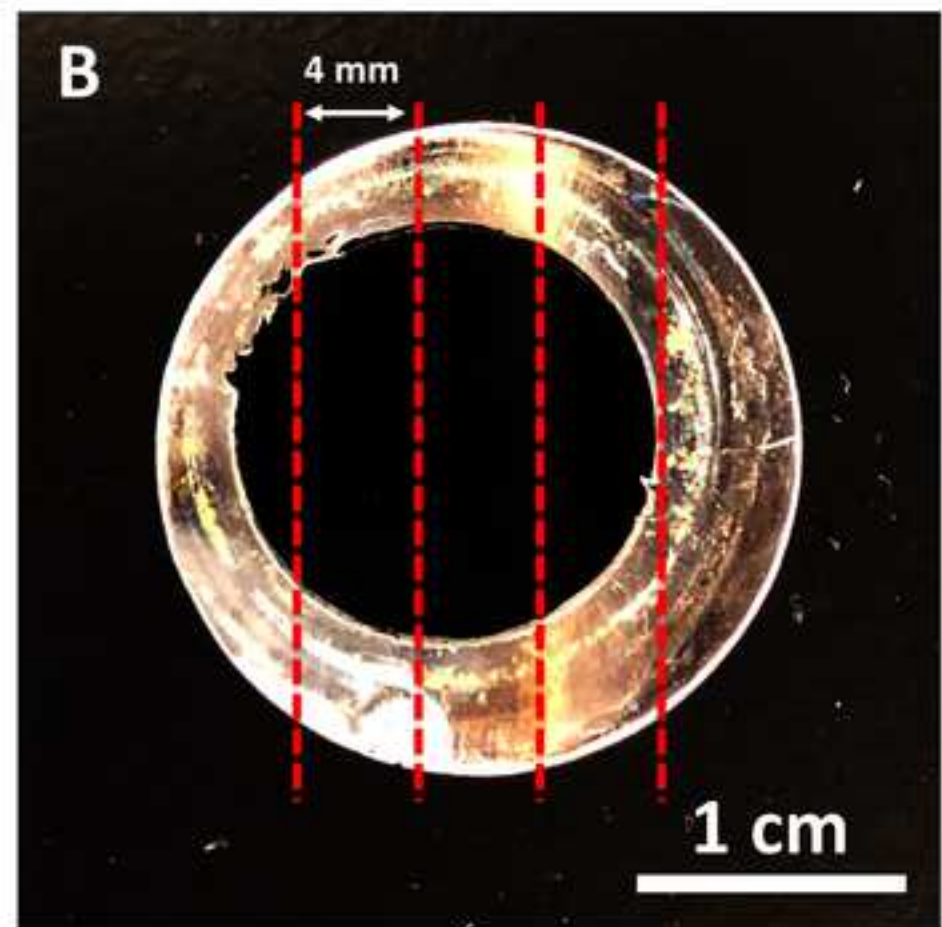
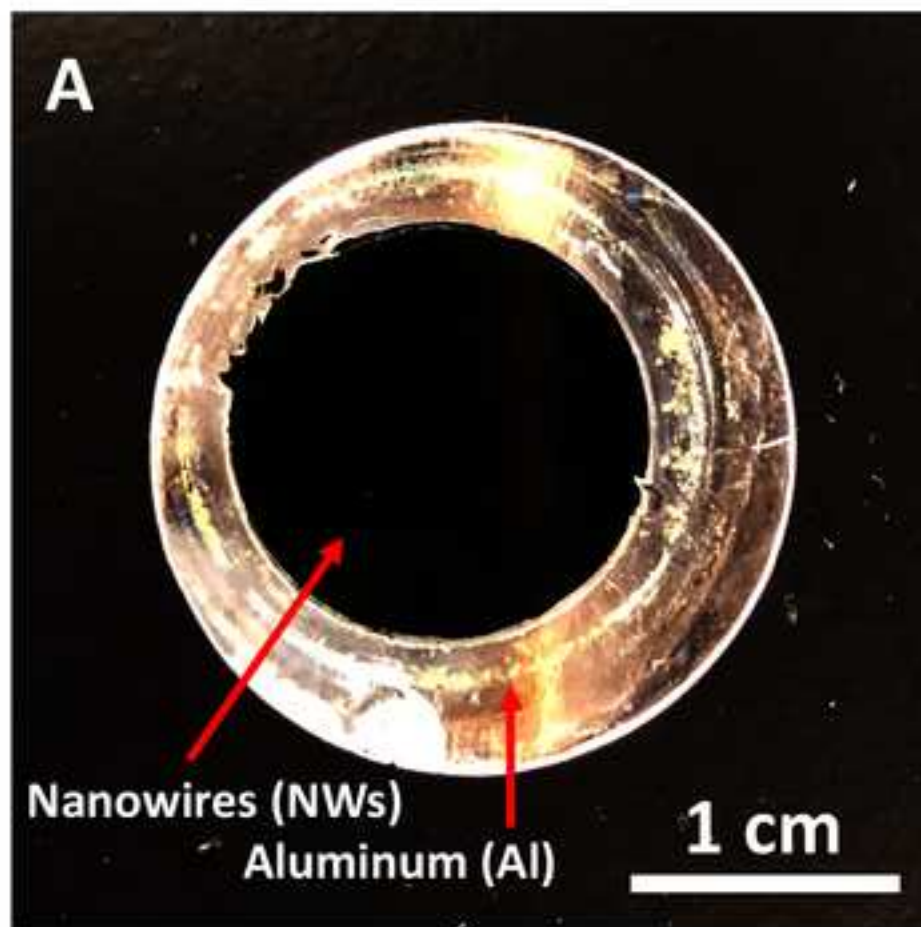
49 Veisheh, O., Gunn, J. W., Zhang, M. Design and fabrication of magnetic nanoparticles for targeted drug delivery and imaging. *Journal of Advanced Drug Delivery Reviews*. **62** (3), 284-304 (2010).

50 Rosenblum, D., Joshi, N., Tao, W., Karp, J. M., Peer, D. Progress and challenges towards targeted delivery of cancer therapeutics. *Nature Communications*. **9** (1), 1410 (2018).

51 Bazak, R., Houri, M., El Achy, S., Kamel, S., Refaat, T. Cancer active targeting by nanoparticles: a comprehensive review of literature. *Journal of Cancer Research Clinical Oncology*. **141** (5), 769-784 (2015).

- 52 Zeilstra, J. et al. CD44 expression in intestinal epithelium and colorectal cancer is independent of p53 status. *PLoS One*. **8** (8), e72849 (2013).
- 53 Pesarrodoná, M. et al. Intracellular targeting of CD44+ cells with self-assembling, protein only nanoparticles. *International Journal of Pharmaceutics*. **473** (1-2), 286-295 (2014).
- 54 Chandra, V. et al. Quantitative assessment of CD44 genetic variants and cancer susceptibility in Asians: a meta-analysis. *Oncotarget*. **7** (45), 74286 (2016).
- 55 Thapa, R., Wilson, G. D. The importance of CD44 as a stem cell biomarker and therapeutic target in cancer. *Stem Cells International*. **2016** (2016).
- 56 Gao, S., Zheng, X., Jiao, B., Wang, L. Post-SELEX optimization of aptamers. *Analytical Bioanalytical Chemistry*. **408** (17), 4567-4573 (2016).
- 57 Das, M., Mohanty, C., Sahoo, S. K. Ligand-based targeted therapy for cancer tissue. *Expert Opinion on Drug Delivery*. **6** (3), 285-304 (2009).
- 58 Janeway, C. A., Travers, P., Walport, M., Shlomchik, M. *Immunobiology: the Immune System in Health and Disease*. Vol. 2 (Garland Pub. New York, 2001).
- 59 Patel, N. S., Lago-Cachón, D., Mohammed, H., Moreno, J. A., Kosel, J. Iron Nanowire Fabrication by Nano-Porous Anodized Aluminum and its Characterization. *Journal of Visualized Experiments*. (152), e60111 (2019).
- 60 Rao, X. et al. High density gold nanoparticles immobilized on surface via plasma deposited APTES film for decomposing organic compounds in microchannels. *Applied Surface Science*. **439**, 272-281 (2018).
- 61 Merck. (3-Aminopropyl)triethoxysilane, <<https://www.sigmaaldrich.com/catalog/product/aldrich/440140?lang=en®ion=SA>> (2020).
- 62 Munguía-Cortés, L. et al. APTES-functionalization of SBA-15 using ethanol or toluene: Textural characterization and sorption performance of carbon dioxide. *Journal of the Mexican Chemical Society*. **61** (4), 273-281 (2017).
- 63 Sperling, R. A., Parak, W. J. Surface modification, functionalization and bioconjugation of colloidal inorganic nanoparticles. *Philosophical Transactions of the Royal Society A: Mathematical & Physical Engineering Sciences*. **368** (1915), 1333-1383 (2010).





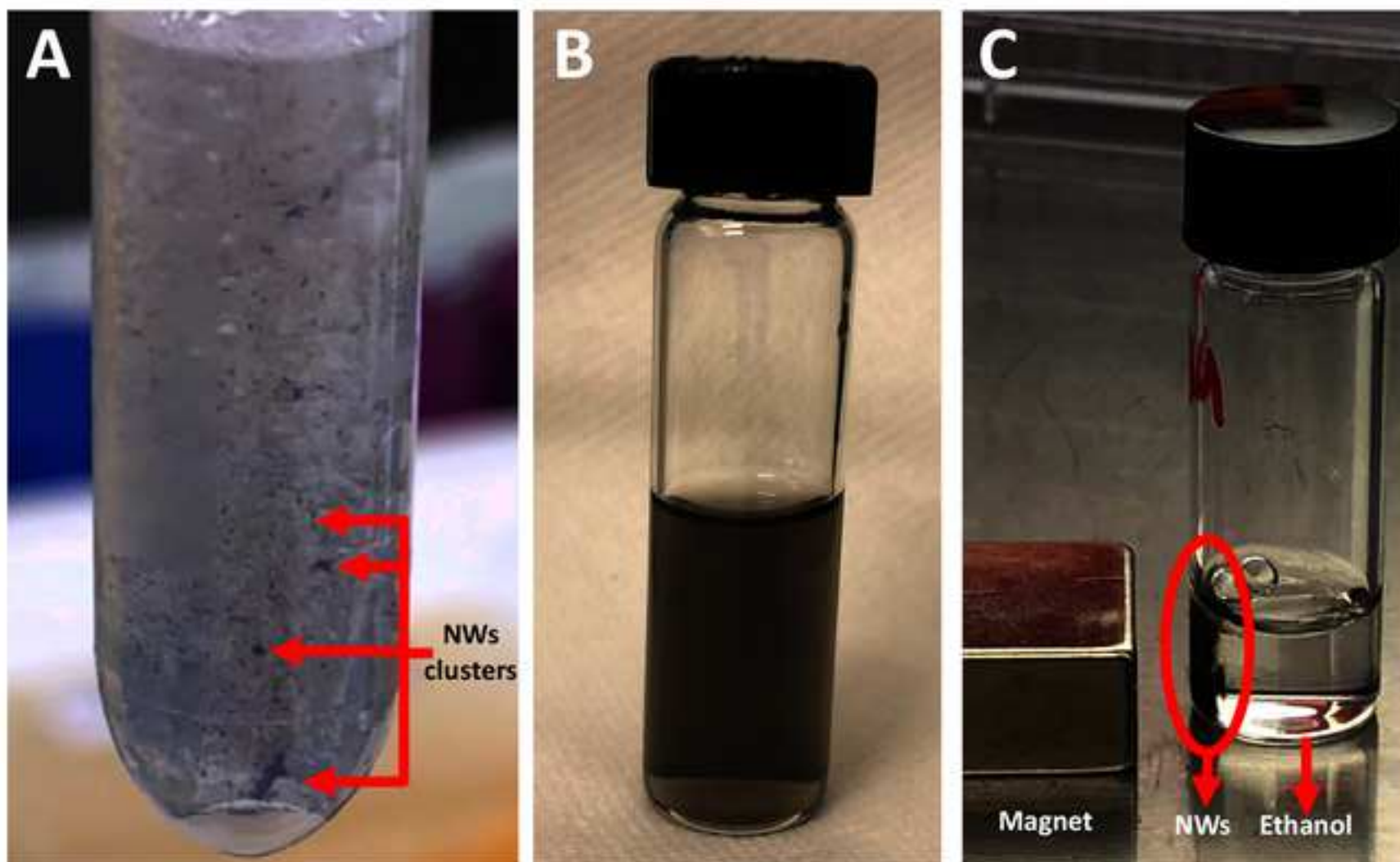
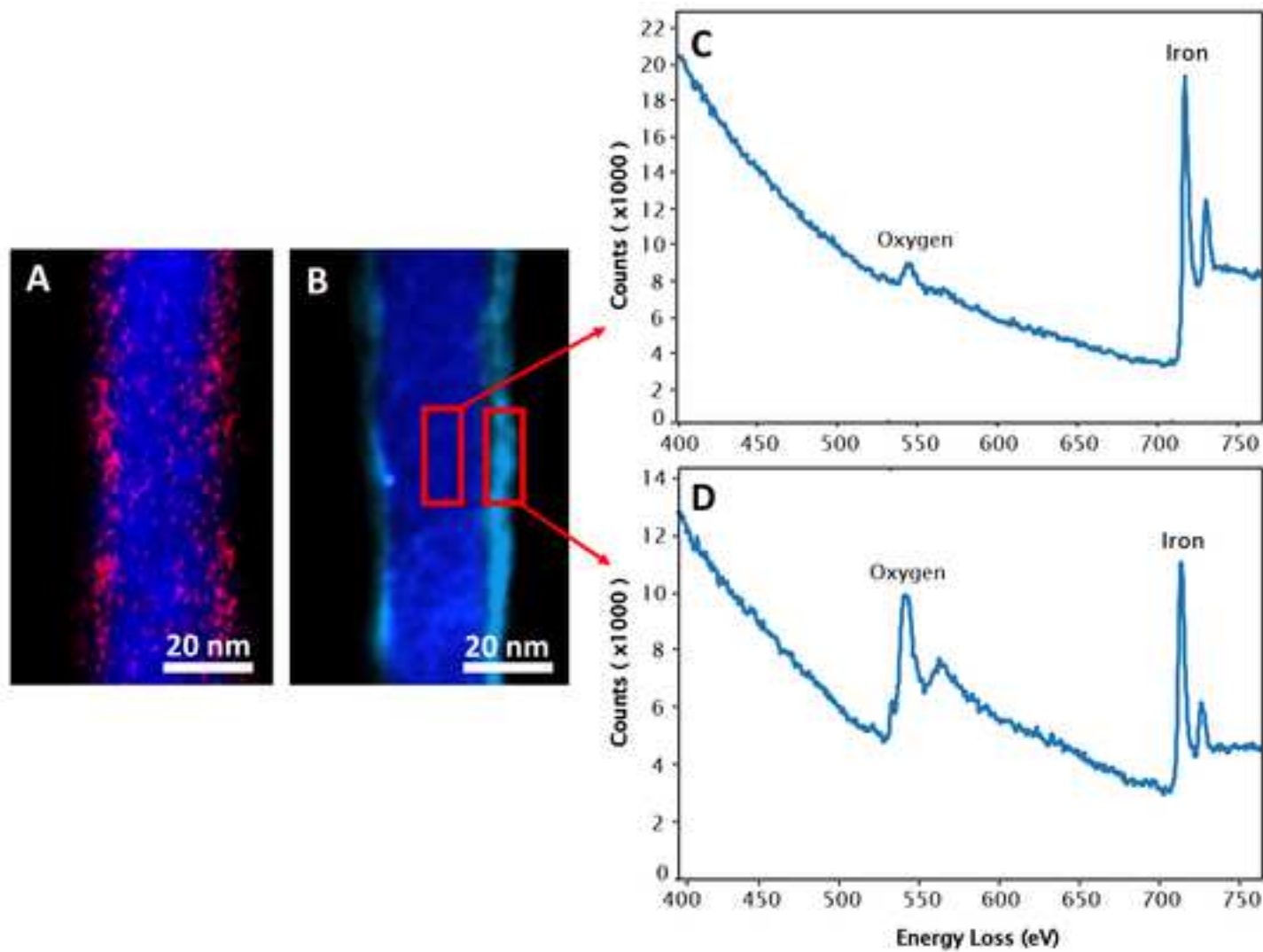





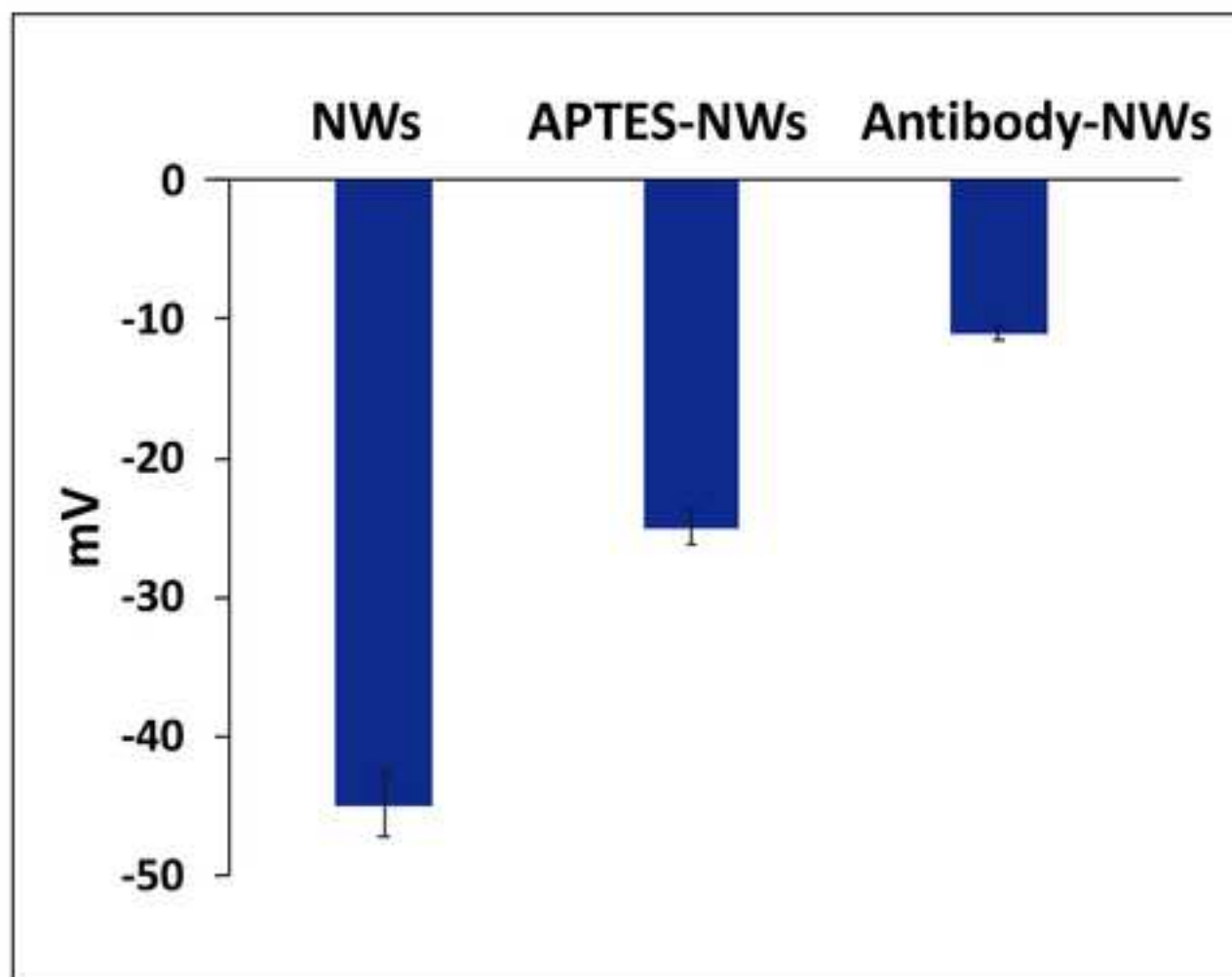
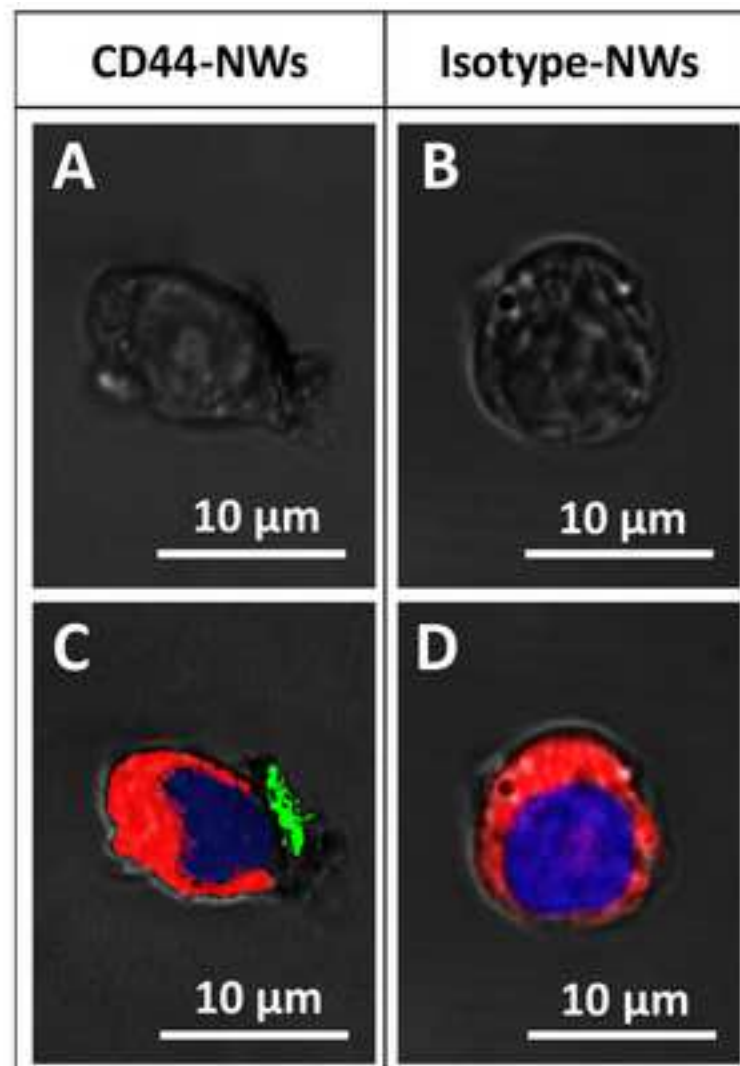


Figure 4



- Ve	- CD44 cells	+ CD44 cells		+Ve
NWs	CD44 NWs	Isotype NWs	CD44 NWs	cell lysate
				





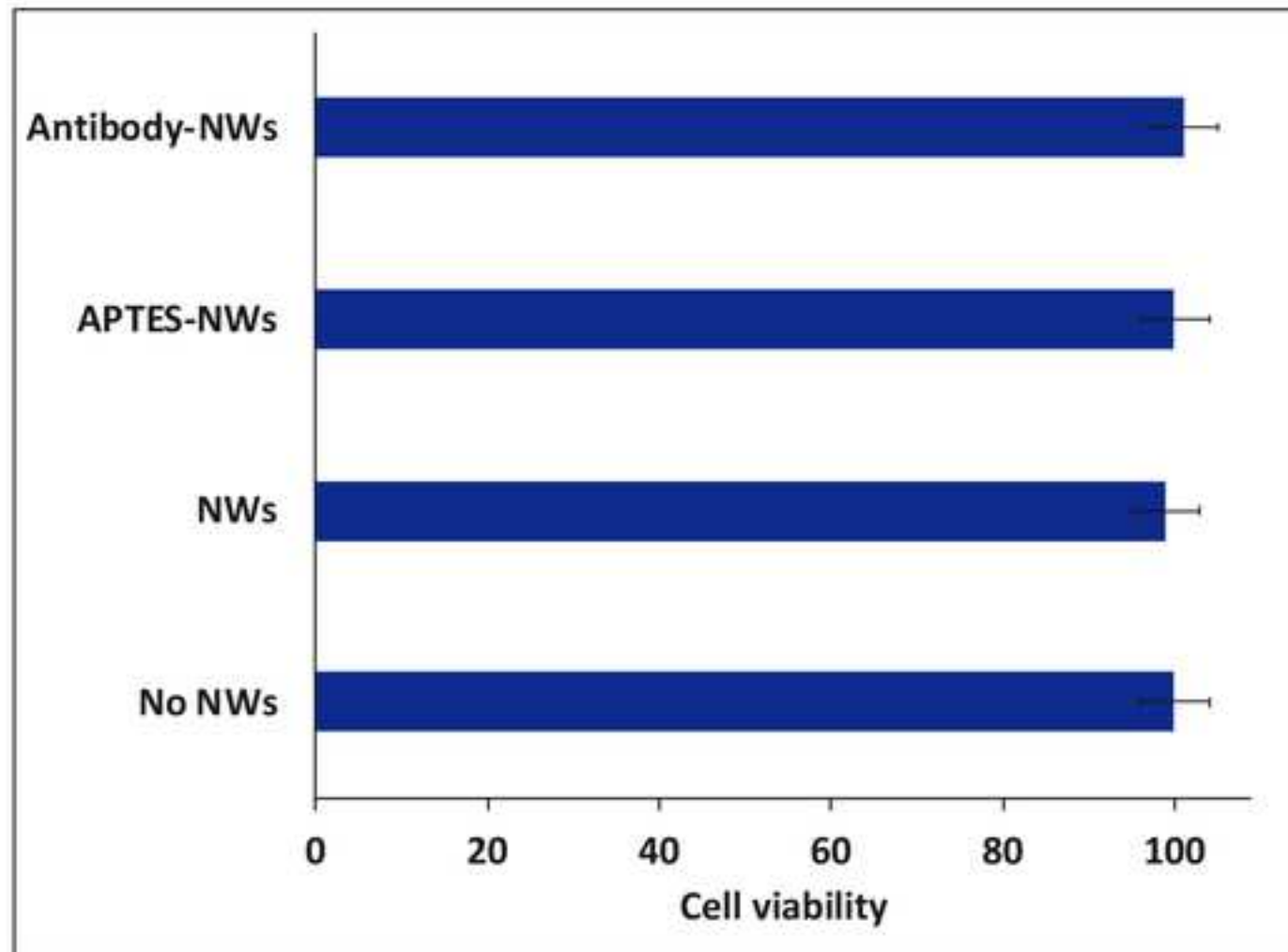


Table 1. Calculating the Fe NW mass

Parameter	Value	Unit
Length of Fe NW (h)	2.6	μm
Radius (diameter/2) (r)	0.01679231	μm
Fe density (D)	7.87	g/cm ³
1 Fe NW volume (V)= π r^2h	2.30E-15	cm ³
1 Fe NW mass = V x D	1.80E-08	μg
1 Fe NW surface area = 2π r^2 + 2πrh	2.76E-01	μm ²

2.8E+05	nm ²
---------	-----------------

Table 2: Calculation the number of APTES molecules required for NWs coating

Parameter	Value
Density of APTES/100 μL *	9.50E-01
Molecular weight (MW) of APTES	2.21E+02
Number of APTES mole = mass/MW	4.29E-03
Number of APTES molecules/100 μL **	2.57E+21
APTES size ***	5.00E-01
APTES surface area	2.00E-01
NW surface area****	2.76E+05
Number of NWs in 0.3mg of NW ****	1.70E+10
Number of APTES molecules needed to create one layer around the NW	1.38E+06
Number of APTES molecules needed for 0.3 mg of NWs	2.35E+16

*Reference number 61

** Number of molecules = Number of mol*avogadro number ($6\text{E}+23$)

***Reference number 62

****From Table 1

Unit
g
g/mol
mol
molecules
nm
nm ²
nm ²
NWs
APTES molecule
APTES molecule

Table 3. Calculating the number of antibodies on nanowire

	Y-shape IgG antibody
Mass for one antibody	2.3E-13 µg
Surface area for one antibody	23 nm ²
Based on BCA assay	0.3 mg
The number of the antibody molecule and NW in 0.3 mg of antibody per mg of NW	~1E+15 antibodies
Number of antibody molecule per NW	~2E+04 antibodies

*Calculated from table 1

** The number of the antibodies in 0.3 mg was calculated by dividing the antibody number that we received by the average molecular weight of Y-shaped IgG antibodies (180 kDa = 3E-16 mg)

***Based on the surface area of one molecule of Y-shaped IgG antibodies (~23 nm²) and the surface area covered by around 1E+04 antibodies would be enough to create a monolayer on the NW. In our case, the density of antibodies is higher than the expected amount. This can be related to the APTES coating that provides more arms that allows the high density of antibodies. This case ensures that the NW is fully covered with the antibodies and the opportunity for the antibody to bind to the cell is high regardless of the orientation of the NWs will be high. However, if the antibody density is lower than the expected amount (of antibody), then the binding chance between the cell and the NWs will be lower.

NW
1.8E-08 μg^*
2.6E+05 nm^2
g per 1 mg
s ** per $\sim 5.6\text{E}+10$ NWs
odies per 1 NW***

from the BSA assay (0.3 mg)
).

of one NW ($\sim 2.6\text{E}+05 \text{ nm}^2$),
 ody was two times more than
 attachment of the antibodies.
 ind to a cell surface antigen,
 sted number ($1\text{E}+04$ molecule
 r.

Name of Material/ Equipment	Company	Catalog Number
2 mL tube (snap-cap Microcentrifuge)	Eppendorf, Fisherscientific	05-402-7
2-N-Morpholino EthaneSulfonic acid hydrate 99% (MES)	Thermoscientific	AC172590250
3-3-Dimethyl-aminopropyl Carbodiimide (EDC)	Thermofisher	PG82079
3-AminoPropyl-Tri-Ethoxy-Silane (APTES)	Sigma Aldrich	919302
5 mL glass tube	Fisherscientific	03-339-22C
96-well plate (flat bottom)	Sigma Aldrich	CLS3595
Anti-CD44 antibody	BD Biosciences	550990
APTES ((3-Aminopropyl)triethoxysilane), 99%	Sigma Aldrich	919-30-2
BCA assay (Pierce BCA Protein Assay Kit)	Thermofisher	23225
Bovine Serum Albumin solution (BSA)	Sigma Aldrich	9048-46-8
Cell incubator	Thermofisher	50116047
Cell viability reagent	AlamarBlue,Thermofisher	DAL1025
Colon cancer cells - HCT116 cell line	ATCC	430641
Hardwood Hammer		
Inductively coupled plasma Mass Spectrometer (ICP-MS)	Perkin Elmer	ELAN 9000 ICP-MS
Laboratory Retort Stand with Clamp	RVFM	13-0140
Magnetic rack (DynaMag-2 Magnet)	Thermofisher	12321D
McCoy's 5A Medium 1x	Gibco	16600082
Microplate reader (Bio-Rad xMark Absorbance Spectrophotometer)	Bio-Rad	1681150
Phosphate buffered saline (PBS) 10x	Gibco	14200067
Phosphate buffered saline (PBS) 1x	Gibco	14190136
Plate shaker (Microplate Genie)	Scientific Industries (Genie)	SI-0400
Single Edge Razor blades	Polysciences	08410-1
Sodium hydroxide (NaOH)	Sigma Aldrich	1310-73-2
Sulfo-N-HydroxySulfosuccinimide (sulfo-NHS)	Thermofisher	106627-54-7
Trypsin	ATCC	30-2101
Tube rotator	VWR	10136-084
Tube shaker (Eppendorf Thermomixer R Mixer, 2.0 mL)	Eppendorf, Fisherscientific	05-400-204
Ultrasonic bath (2510)	Branson	2489502

Comments/Description
Concentration 0.1 M and pH 4.7
Clone 515, concentration 1 mg/mL
Concentration 99%
Concentration 35%
Any hammer tool can be used, there is no specific brand.
The used software is "Elan instrument control session"
This is used to handle the 5 mL glass tube in the sonicator bath.
Microplate Manager 6 software (#168-9520)
Concentration 0.1 M (No calcuim, no magnesium)
Concentration 0.01 M (No calcuim, no magnesium)
Concentration 1 M, pH 13

Manuscript number: VE61360
Response to Reviewers

Dear Dr. Nam Nguyen,

Thank you for giving us the opportunity to submit a revised draft of the manuscript “Biofunctionalization of Magnetic Nanomaterials” for publication in the Journal of JOVE. We appreciate the time and effort that you and the reviewers dedicated to providing feedback on our manuscript. We have incorporated the suggestions made by you. Please see below, in blue, for a point-by-point response to your comments and concerns.

1. Please highlight up to 2.75 pages of protocol text in the current manuscript to ensure that videography can occur in a single day. This is a hard production limit.

Author response: Thank you for pointing this out. The essential steps have been highlighted so the number of the highlighted steps is not more than 2.75 pages.

2. Please provide a complete reference for reference 23.

Author response: Thank you for pointing this out. This reference has been replaced with an appropriate one with a complete format.